UAB
Universitat Autònoma de Barcelona

Dipòsit digital de documents de la UAB

This is the **accepted version** of the journal article:

Pujol, Lluís; Sánchez Cabeza, Joan Albert. «Determination of longitudinal dispersion coefficient and velocity of the Ebro river waters (Northeast Spain) using tritium as a radiotracer». *Journal of Environmental Radioactivity*, Vol. 45, Num. 1 (October 1999), p. 39-57 DOI 10.1016/S0265-931X(98)00075-7

This version is available at https://ddd.uab.cat/record/326141

under the terms of the BY-NC-ND license.

Determination of longitudinal dispersion coefficient and velocity of the Ebro river waters (Northeast Spain) using tritium as a radiotracer

Ll. Pujol and J.A. Sanchez-Cabeza

Departament de Física, Universitat Autònoma de Barcelona, ES-08193 Bellaterra, Barcelona, Spain

ABSTRACT

Tritium routinely released as low-activity liquid radioactive waste by the Ascó nuclear power plant (Tarragona, Spain) was used as a radiotracer to determine the longitudinal dispersion coefficient and velocity of the Ebro river waters (Northeast Spain). Several field experiments, in co-ordination with the nuclear power plant, were carried out during 1991. After a tritium release, water was sampled downstream at periodic intervals during several hours. Tritium was measured with a low-background liquid scintillation counter and the time evolution of its concentration for different locations was obtained. In order to determine the longitudinal dispersion coefficient and the velocity of the Ebro river waters, experimental data were fitted using an analytical, a box–type and a numerical model to solve the one-dimensional advection-diffusion equation. Observed mixing length occurred about 50 channel widths downstream from the point source, shorter than values predicted from some published expressions (100 – 300 channel widths). For the river water flows investigated, ranging from 178 to 915 $m^3\ s^{-1}$, longitudinal dispersion coefficients ranged from 41 ± 30 to 392 ± 45 $m^2\ s^{-1}$ and mean velocities ranged from 0.563 ± 0.011 to 1.278 ± 0.019 m s^{-1}.

INTRODUCTION

The hydrosphere constitutes an important medium by which pollutants can be dispersed in the environment and incorporated to the food chains. Consequently, knowledge of the hydrological characteristics of the aquatic environment in which pollutants can be transported is a first step towards the formulation of a complete description of the phenomenon through models (Wicker & Schultz, 1982; Eisenbud, 1987; Sanchez-Cabeza *et al*., 1992).

The advection-diffusion equation is adequate to describe the dispersion of conservative pollutants in, amongst other systems, porous media, rivers and channels. The dispersion process of a pollutant into a river can be divided into three phases (Yotsukura & Sayre, 1976; IAEA, 1985; Scott, 1994):

1. Initial mixing: the effluent (or tracer) is discharged into the river with an initial momentum and is not fully mixed. This phase extends from the source to a section where the distribution of tracer concentration becomes uniform over depth, and may cover a distance of up to about one hundred times the depth of the river channel. In this first stage three-dimensional equations are needed to study the dispersion.
2. Full mixing: the effluent has lost its initial momentum and mixing is complete. This stage extends from the end of the initial mixing zone to a section where the tracer is mixed over the full cross-section of the water body, and may cover from 3 to 10 km in large rivers. To model this stage one- or two-dimensional equations may suffice.
3. Far field dispersion: this stage extends from the end of the full mixing zone to a long distance, where the tracer concentration may become undetectable. The distance from the source to the point in which mixing is homogeneous and complete is known as the mixing length. One-dimensional equations may be used to model this

phase. Apart from convective transport, the predominant effect in this stage is longitudinal dispersion, that is, tracer cloud stretching in the velocity direction.

One of the important assumptions of the tracer dilution principle in the third stage is full mixing. In this case, and also for a continuous release under stationary hydraulic conditions, the tracer activity in the river (C_o) can be calculated as

$$C_o = \frac{C_t}{Q}\, q \tag{1}$$

where C_t is the mean concentration of tracer release, q is the flow rate of the tracer discharge and Q is the river discharge. This is valid for sampling points located at a distance from the source greater than the mixing length. A number of empirical formulae have been proposed to estimate the mixing length (L):

1. Day (1977)

$$L = 25w \tag{2}$$

where w is the channel width.

2. Hull (Guizerix & Florkowski, 1983): this empirical formula is based on experience in gauging numerous rivers but in general underestimates the mixing length:

$$L = \sqrt{\frac{w^3}{d}} \tag{3}$$

where w and d are the channel width and mean depth, respectively.

3. Rutherford (1994)

$$100w < L < 300w \tag{4}$$

where w is the channel width.

Nevertheless, these expressions should be used with caution as they have been empirically established for particular rivers. In the case of the Ebro river, the mixing length computed using eqns (2) and (3) in the area comprised between Ascó and Pas de l'Ase, is 2 km and 5 km, respectively, in agreement with the observation of full heat mixing at 6.5 km from the release point (Asociación Nuclear Ascó, personal communication, 1990). Although the mixing length computed using eqn (4) is from 12 km to 42 km, we assumed far-field radionuclide dispersion from a point source in a river system using the one-dimensional advection-diffusion equation. In this case, it can be assumed that the tracer was mixed in the river cross-section after the mixing length. This assumption will be studied in the Discussion section comparing the total amount of tritium released by the nuclear power plant and the total amount observed at each sampling location.

In the far field zone, the one-dimensional advection-diffusion equation is expressed as (Fischer, 1973; Lebreton, 1974; Day, 1975; Beltaos, 1980; Nordin & Troutman, 1980):

$$\frac{\partial c(x,t)}{\partial t} = D\frac{\partial^2 c(x,t)}{\partial x^2} - v\frac{\partial c(x,t)}{\partial x} \tag{5}$$

where $c(x,t)$ is the concentration of the pollutant, D is the longitudinal dispersion coefficient and v is the mean flow velocity. Even though the velocity is relatively easy

to measure by other means, this is not the case for the dispersion coefficient.

Longitudinal dispersion arises principally as a result of transverse velocity shear. The longitudinal dispersion coefficient can be estimated from the velocity distribution. This approach was first developed by Taylor in an expression to calculate the longitudinal dispersion coefficient in pipes (Fischer, 1973; Lebreton, 1974; Day, 1975; Beltaos, 1980; Nordin & Troutman, 1980; Rutherford, 1994):

$$D = 10.1ru^* \tag{6}$$

where r is the pipe radius and u^* is the shear velocity. Taylor's expression was used to calculate longitudinal dispersion coefficients in channels and rivers, but these were only approximate because of the difference between the velocity geometric distribution in a pipe and in a channel or a river. For example, Elder (1959) considered that in a river the mean depth was the only important parameter, and developed a similar expression to that of Taylor (Lebreton, 1974; Beltaos, 1980; Rutherford, 1994):

$$D = 5.93du^* \tag{7}$$

where d is the mean depth. Thereafter, Fisher extended this method, considering that the dominant scale was the mean width instead of the depth. The approximate expression of his model can be written as (Fischer, 1973; Rutherford, 1994):

$$D = \frac{Iw^2\overline{u'^2}}{k_z} \tag{8}$$

where I is a dimensionless parameter which quantifies the velocity variation over the cross-section (normally $I = 0.07$), w is the channel width, k_z is the transverse dispersion coefficient, and u' is the velocity deviation from the local depth-averaged velocity. The overbar denotes the mean square over the cross-section. The application of eqn (8) is not immediate since (Lebreton, 1974; Rutherford, 1994):

- The transverse dispersion coefficient varies significantly between channels and throughout a given channel, and the uncertainties in estimating k_z from the literature are large.
- It is necessary to determine the spatial distribution of the transverse velocity, requiring difficult and costly sampling.

The application of eqns (7) and (8) to flows in natural channels has met with mixed success (Fischer, 1973; Lebreton, 1974; Day, 1975). The discrepancies between theoretical and field results are not surprising as natural channels probably never meet the required assumptions of uniform cross section, steady flow, and constant mass balance (Day, 1975). In conclusion, the most convenient method to determine the longitudinal dispersion coefficient in rivers is experimentally using a tracer (Lebreton, 1974; Rutherford, 1994).

Tracers are used to obtain information from a system by observing the behaviour of a specific substance (tracer) that has been added to the system. There are three main types of tracers used in water research: chemical, fluorescent or radioactive (Guizerix & Florkowski, 1983; ISO, 1987; Gordon *et al*., 1992). In most field studies the longitudinal dispersion coefficient is determined by the use of chemical or fluorescent tracers (Day, 1975; Mossman *et al*., 1991; Graf, 1995; Clark *et al*., 1996), although they present different problems. For example, Rhodamine WT dye, the tracer most

commonly used, presents numerous drawbacks as (*i*) it decomposes in sunlight, (*ii*) degradation products can be toxic, *(iii)* it adheres to sediments, and (*iv*) it is relatively expensive (Graf, 1995; Clark *et al*., 1996).

In this study, tritium routinely released as low-activity liquid radioactive waste by the Ascó nuclear power plant (Tarragona, Spain), was used as a radiotracer to determine the longitudinal dispersion coefficient and the velocity of the Ebro river waters (Northeast Spain). This was possible by the use of a rapid and sensitive technique for the detection of low tritium concentrations in river waters. The advantages of the use of tritium were numerous: (*i*) it is an ideal water tracer as it forms tritiated water molecules, (ii) it does not adsorb to sediments, (*iii*) sampling is easy and it does not require special techniques, (*iv*) small sample amounts can be used and extremely low tritium concentrations in water can be measured by liquid scintillation, and (*v*) the relatively long half-life of tritium ($T_{1/2}$ = 12.43 years) enables it to be stored before being measured (Guizerix & Florkowski, 1983).

MATHEMATICAL MODELLING

Pollutants dispersion in surface waters can be modelled using analytical, box-type and numerical solutions (IAEA, 1985; Scott, 1994). We solved the transport equations for each type of model.

Analytical model

The boundary conditions required to solve analytically the one-dimensional advection-diffusion equation in our case were the following:

- The tritium pulsed release was described as a step function:

$$c(x,0) = C_i \tag{9}$$

$$c(0,t) = \begin{cases} C_0 & 0 < t \le t_0 \\ 0 & t > t_o \end{cases} \tag{10}$$

- To avoid any effect of the downstream boundary on results, a semi-infinite flow line was assumed for the model (Knopman & Voss, 1987):

$$\frac{\partial c}{\partial x}(\infty,t) = 0 \tag{11}$$

Then, the analytical solution to the one-dimensional advection-diffusion equation was the following (Van Genuchten & Alves, 1982):

$$c(x,t) = \begin{cases} C_i + (C_0 - C_i)A(x,t) & 0 < t \le t_0 \\ C_i + (C_0 - C_i)A(x,t) - C_0 A(x,t-t_0) & t > t_0 \end{cases} \tag{12}$$

where

$$A(x,t) = \frac{1}{2}\operatorname{erfc}\left[\frac{x - vt}{2(Dt)^{1/2}}\right] + \frac{1}{2}\mathrm{e}^{-\frac{vx}{D}}\operatorname{erfc}\left[\frac{x + vt}{2(Dt)^{1/2}}\right] \tag{13}$$

and erfc (x) is the complementary error function (Abramowitz & Stegun, 1972; Press *et al.*,1986).

Box-type model

The time evolution of the number of atoms of a given radionuclide in a compartment i is given by (Abril & García León, 1992):

$$\frac{\mathrm{d}}{\mathrm{d}t}N_\mathrm{i} = -k_{\mathrm{i},1}N_\mathrm{i} + k_{\mathrm{i}+1,2}N_{\mathrm{i}+1} + k_{\mathrm{i}-1,1}N_{\mathrm{i}-1} - k_{\mathrm{i},2}N_\mathrm{i} + Q_\mathrm{i}(t) - \lambda N_\mathrm{i} \tag{14}$$

where $Q_\mathrm{i}(t)$ includes all the sources of radionuclides in the system and λ is the tritium radioactive decay constant. In our case, the radioactive decay constant term, λN_i, is negligible due to the rapidity of the phenomenon compared to the tritium half-life. The transfer coefficients between two adjacent compartments are given by the following expressions:

$$k_{\mathrm{i},1} = \frac{v_\mathrm{i}S_\mathrm{i}}{V_\mathrm{i}} + \frac{k_\mathrm{b}S_\mathrm{i}}{\Delta x_\mathrm{i}V_\mathrm{i}} \tag{15}$$

$$k_{\mathrm{i},2} = \frac{k_\mathrm{b}S_\mathrm{i}}{\Delta x_\mathrm{i}V_\mathrm{i}} \tag{16}$$

where $k_{\mathrm{i},1}$ is the transfer coefficient from compartment i to compartment i+1, $k_{\mathrm{i},2}$ is the transfer coefficient from compartment i to compartment i-1, k_b is a dispersion coefficient, V_i is the volume of the compartment *i*, S_i is the surface of the compartment *i* and Δx_i is the length of the compartment *i*. The first term on the right hand of eqn (15) refers to the convective term and the second to the dispersion term. In eqn (16) only dispersion is considered since there is no flow upstream (Abril & García León, 1992).

The water volume exchanged by a compartment i during Δt must be smaller than the volume, V_i, of the compartment. Mathematically, this can be expressed as: $\Delta t << 1/k_{max}$. On the other hand, the hypothesis of instantaneous and homogeneous mixing of a radionuclide input in a compartment produces numerical dispersion during calculation. This effect is equivalent to adding k_b' to the dispersion coefficient k_b according to the expression (Prandle, 1984)

$$k_b' = \frac{1}{2}(v\Delta x - v^2\Delta t) \tag{17}$$

Then, the longitudinal dispersion coefficient from eqn (5) is expressed as

$$D = k_b + k_b' \tag{18}$$

It can be shown that numerical dispersion presents a minimal value (Pujol, 1996):

$$k_{b\,\min}' = \frac{1}{2}\left(\frac{1}{v\,\Delta x} + \frac{1}{k_b}\right)^{-1} \tag{19}$$

There are two conditions for which the determination of the dispersion coefficient (D) is not possible: i) if $k_b' < k_b'_{min}$, the solution is unstable, and ii) if $k_b' > D$, the value of k_b is indefinite.

The optimisation of the spatial and temporal resolution led us to choose Δx = 100 m and Δt = 15 s, or Δx = 250 m and Δt = 60 s, depending on the distance to the release point. For these grids, the solution of eqn (5) was stable.

Numerical model

The solution of the one-dimensional advection-diffusion equation using an explicit finite differences method can be obtained from the following expression:

$$c_{x,t+\Delta t} = \left(\frac{D\Delta t}{(\Delta x)^2} - \frac{v\Delta t}{\Delta x} \right) c_{x+\Delta x,t} + \left(1 - 2\frac{D\Delta t}{(\Delta x)^2} + \frac{v\Delta t}{\Delta x} \right) c_{x,t} + \frac{D\Delta t}{(\Delta x)^2} c_{x-\Delta x,t} \qquad (20)$$

where $c_{x,t+\Delta t}$ is the mean cross sectional concentration as a function of time for a distance x from the emission point. The stability of eqn (20) can be analyzed using the Fourier method (Kincaid & Cheney, 1991). Thus, this equation is stable if:

$$\left(1 - 2\left(2\frac{D\Delta t}{(\Delta x)^2} - \frac{v\Delta t}{\Delta x} \right) sin^2\left(\frac{\theta}{2} \right) \right)^2 + \left(\frac{v\Delta t}{\Delta x} sin(\theta) \right)^2 \leq 1 \quad \forall \ \theta \in \{0,\ 2\pi\} \qquad (21)$$

The optimisation of the spatial and temporal resolution led us to choose Δx = 100 m and Δt = 15 s, respectively, for which the solution is stable (Pujol, 1996).

EXPERIMENTAL SECTION

Study area and sampling

The Ebro river is located in the Northeast of Spain and discharges into the Mediterranean sea after flowing for more than 900 km. The Ascó nuclear power plant is established in the final section of the river and comprises two pressurized-water reactor (PWR) units: Ascó I and Ascó II (Fig. 1). During their normal operation, these two units

generate low-activity radioactive liquid waste, including tritium, which is released into the river in a controlled way: most activity is released from storage tanks, although a continuous release also exists. This routine operation can be used to trace river waters downstream.

In order to study the hydrological dispersion of conservative pollutants in the Ebro river waters, seven tank releases were followed at different locations during 1991, in co-ordination with the Ascó nuclear power plant. The characteristics of each release are shown in Table 1. In the chosen location, water was sampled from the river every 15 minutes during a total sampling period which ranged from 4 to 8 hours, depending on the distance to the nuclear power plant and the river flow (Table 2). Special attention was given to the collection and preservation of samples (Keith *et al*., 1983; APHA-AWWA-WEF, 1992). Samples were collected in 125 ml polyethylene bottles, which had been carefully washed in the laboratory before each sampling campaign. Water was collected above the riverbed and sufficiently far from the border, natural or artificial obstacles, and avoiding stagnant or turbid water zones. Before the sample was collected, containers were rinsed three times with flowing river water. Simultaneous sampling collection from differents points in the same cross-section at each sampling site was discarded because it was assumed that the tracer was fully mixed in the river cross-section after the mixing length. Finally, samples were taken to the laboratory for their analysis.

Analysis

As tritium is a soft beta emitter (5.72 keV mean energy), liquid scintillation is the most appropriate technique for its measurement. In this work, the low-background liquid scintillation spectrometer Quantulus 1220 was used to determine tritium in river water

samples (Pujol, 1996).

The analytical method used to determine tritium in river water samples was, briefly, the following: (*i*) samples were filtered through slow depth filters (such as Whatman 542), (*ii*) 8 ml of the filtrate was mixed and vigorously shaken during one minute with 12 ml of the scintillation cocktail OptiPhase Hisafe 3 (Wallac) in polyethylene vials (Wallac), (*iii*) three background samples and three tritium standards were simultaneously prepared, (*iv*) samples, backgrounds and tritium standards were stored in the liquid scintillation spectrometer during at least one day so that the chemiluminescence spectrum, which interferes with tritium measurements, had sufficiently decreased, and (*v*) samples, backgrounds and tritium standards were counted using Quantulus 1220 (Wallac). For a counting time of only 360 min, the detection limit was 2.6 Bq l^{-1} (Currie, 1968) and the analytical uncertainties ranged from 5% to 30% (Pujol, 1996).

RESULTS AND DISCUSSION

Field study

The evolution of tritium concentration in the Ebro river waters after each monitored pulse during 1991 is shown in Fig. 2. Uncertainties were derived from sample preparation and counting statistics. Marks without errors bars correspond to detection limits. Some observations were lower than the detection limit of 2.6 Bq l^{-1} because some samples were measured more than 360 minutes. All reported uncertainties correspond to $\pm 1\sigma$. A tritium concentration maximum was clearly observed for all field experiments (except Fig. 2C, Mora de Ebro August 5, 1991), and showed a variable amplitude and time, depending on the total tritium activity released by the nuclear power plant, the river discharge and the distance from the source. Singular

characteristics can be observed in some of the field experiments:

- Ascó, December 9, 1991 (Fig. 2E): the peak presented a flat response during about 50 minutes. This was due to the fact that dispersion had not yet affected the central part of the pulse at short distances from the plant. In fact, this location was closer to the source than the mixing length, so results were not used to fit the mathematical models.
- Mora de Ebro, December 5, 1991 (Fig. 2D): the tritium peak showed a long-tail. This could be partly explained by river discharge variations during the sampling period producing different mean water velocities. However, this phenomenon is usually attributed to the irregular shape of the riverbed, which may produce water dead zones that cause tracer retention (Day, 1975; Nordin & Troutman, 1980; Yu & Wenzhi, 1989; Rutherford, 1994). The same behaviour was clearly observed in Miravet, December 16, 1991.
- Mora de Ebro, August 5, 1991 (Fig. 2C): the peak was not fully observed as the sampling period, determined *a priori* from limited knowledge, was not adequate. For this reason, these results were not used to fit the mathematical models. On the other hand, the tritium maximum was superimposed on a background level of approximately 20 Bq l^{-1}. This may indicate the detection of continuous tritium release from the nuclear power plant or the presence of other tank releases close in time. Maximum tritium concentration was larger than the mixing activity (Table 1). This was also the case for García, July 15, 1991 (Fig. 2B). Both experiments were carried out in summer, when river discharges were low. These observations would indicate a certain degree of tracer accumulation in river waters or incomplete mixing at these locations when discharge is low.

Longitudinal dispersion coefficient and velocity were the two hydrological

parameters necessary for the description of the movement and dispersion of tritium after the mixing length. They were determined by fitting the solutions of each model with the experimental data, except for the cases mentioned above (Ascó, December 9, 1991 and Mora de Ebro, August 5, 1991).

Longitudinal dispersion coefficient and mean velocity

Several computer codes were written to generate solutions of the advection-diffusion equation for each model and for any parameter values (longitudinal dispersion coefficient and mean velocity). For each solution and measured pulse, chi-square (χ^2) was computed using the following expression:

$$\chi^2 = \sum_{i=1}^{k} \frac{(F_i - \phi_i)^2}{\phi_i} \tag{22}$$

where F_i are the experimental data and ϕ_i are the theoretical values obtained from each model. The fitted solution was obtained by minimisation of χ^2 varying both D and v, and was considered statistically acceptable if $\chi^2 \leq \chi^2_\varepsilon$, where χ^2_ε is the decision limit with an ε significance level, usually chosen as $\varepsilon = 0.05$ (Cuadras, 1991). The fitted functions were also represented, except for Ascó (December 9, 1991) and Mora de Ebro (August 5, 1991) (Fig. 2).

Fitted parameter uncertainties

The parameter uncertainties were determined as briefly explained below (Myers, 1986; Rawlings, 1988). Let us consider a set of experimental data: x_i (independent variable), y_i

(dependent variable) and i = 1, 2,..., n (experimental observations). These data were fitted to a function such that $y_i = f(x_i, \alpha, \beta)$, where α and β are two parameters estimated through the chi-square test. Then, the uncertainties associated to each parameter (σ_α and σ_β) were determined by computing the square root of the diagonal elements of the matrix $s^2(W'W)^{-1}$, where

$$s^2 = \frac{\sum (y_i - \hat{y}_i)^2}{n-2} \tag{23}$$

being s the standard deviation and $\hat{y}_i$ the dependent variable estimator. The matrix $(W'W)^{-1}$ is the covariance matrix, and W' is the transposed matrix of W. The elements of matrix W are defined as:

$$w_{ji} = \left(\frac{\partial f(x_i, \theta_j)}{\partial \theta_j} \right) \tag{24}$$

where θ_j are the parameter estimate ($\theta_1 = \alpha$, $\theta_2 = \beta$). The derivatives were evaluated for the fitted parameters.

In our case:

$$s^2 = \frac{\sum \left(c_i^{\exp} - c_i^{the} \right)^2}{n-2} \tag{25}$$

being $c_i^{\exp}$ the experimental tritium concentration for the i observation and c_i^{the} its theoretical concentration for one of the models used. As $c_i^{the} = f(t, D, v)$, the matrix W was computed as follows:

$$W = \begin{pmatrix} \frac{\partial f(t_1, D, v)}{\partial D} & \frac{\partial f(t_1, D, v)}{\partial v} \\ \frac{\partial f(t_2, D, v)}{\partial D} & \frac{\partial f(t_2, D, v)}{\partial v} \\ \cdots & \cdots \\ \frac{\partial f(t_n, D, v)}{\partial D} & \frac{\partial f(t_n, D, v)}{\partial v} \end{pmatrix}_{(D_o, v_o)} \quad (26)$$

where D_o and v_o are the optimized parameters of longitudinal dispersion coefficient and velocity determined with the different models.

Discussion

A comparison of the total amount of tritium released by the nuclear power plant and the total amount that passed by each sampling location is shown in Table 3. Only in one experiment (Ascó, December 9, 1991), values were significantly different, as the sampling location was before the mixing length. In the other cases small discrepancies can be justified in terms of incomplete pulse observed, tracer retention in dead zones and/or variable tritium background in river waters. Therefore, the assumption of complete mixing after Pas de l'Ase and the use of a one-dimensional transport model was justified. As a consequence, in this area, we may conclude that the observed mixing length was lower than 50 channel widths, which may be compared with the interval 100 – 300 channel widths reported in the literature (Rutherford, 1994).

The fitted values of the longitudinal dispersion coefficient and mean velocity for each field experiment and model are shown in Table 4. The longitudinal dispersion coefficient showed great variability, as it ranged from 41 ± 30 to 392 ± 45 $m^2\ s^{-1}$, largely depending on distance from the sampling location. Although the fitted values for each experiment were similar for all models, values obtained with the numerical model were, in general, higher than those obtained with the analytical and box-type models.

The accuracy in the solution of the partial differential equation depends on the finite difference method used. In our case, a backward space differencing was used in the discretisation of eqn (5), then numerical diffusion always involve additional diffusion as explained by Noye (1987).

The fitted mean velocity for all sampling campaigns showed limited variation, as it ranged from 0.558 ± 0.011 to 1.278 ± 0.019 m s^{-1}, largely depending on river discharge. The fitted mean velocity obtained for the three models, for each experiment, were statistically indistinguishable.

In general, model fittings were satisfactory, although Mora de Ebro December 5, 1991 and Miravet December 16, 1991 showed larger χ^2 than the other field experiments. This was a consequence of the long tail observed in the tritium pulses (Fig. 2). Several authors have successfully proposed a dead zone model in which a term is added to the one-dimensional diffusion equation to allow for temporary entrapment of portions of the tracer in the dead zones (Nordin & Troutman, 1980; Yu & Wenzhi, 1989).

For rivers with similar characteristics to the Ebro river (mean width between 120 - 140 m and mean depth between 2.4 - 3.0 m), similar values of the longitudinal dispersion coefficient were observed (Table 5). However, such comparison is only qualitative, as published values of the longitudinal dispersion coefficient do not include, commonly, uncertainty calculations (Fischer, 1973; Nordin & Troutman, 1980; Mossman *et al*., 1991; Rutherford, 1994; Graf, 1995).

The relation between mean water velocity and river discharge can be described with a power function (Fig. 3), which is useful to estimate transit times if discharge is known. Other authors have also successfully assumed a power function relationship (Knighton, 1984; Morisawa, 1985).

Longitudinal dispersion coefficient in rivers depends on several factors; for instance, distance from the release point, river discharge, mean depth, shear velocity, channel width and dead zones (Day, 1975; Nordin & Troutman, 1980; Rutherford, 1994). In this study, the variation of the longitudinal dispersion coefficient with distance from the release point showed two distinct zones

1. From Ascó to García (0-10.5 km from the release point): the longitudinal dispersion coefficient at Pas de l'Ase and García (ranging from 41 ± 30 to 175 ± 26 $m^2 s^{-1}$) was relatively low.
2. From García to Miravet (10.5-28 km): larger longitudinal dispersion coefficients were observed (ranging from 218 ± 34 to 392 ± 45 $m^2 s^{-1}$). Both peaks at Mora de Ebro and Miravet showed long tails which indicated the presence of dead zones in this section. This is due to the increase of width channel and the decrease of river depth, including island deposition (Knighton, 1984).

In eqn (5) *D* is assumed to be constant, which reduces complexity of the solutions and, in this study, permitted the comparison of the various approaches to solve the proposed problem. However, this was not the case, as the coefficient is largely dependent on river morphology. Although dispersion was studied for several distances from the release point, it was not possible to establish either a relationship between dispersion and distance, as the dispersion coefficient was obtained for different discharges, or between dispersion and river discharge, as the dispersion coefficient was obtained for different reaches. Therefore, future studies are required to carry out the experiment at different locations with constant river discharge and also in the same location for a range of river discharges.

CONCLUSIONS

The best technique to determine the longitudinal dispersion coefficient of a river is through the use of tracers. Experimental data and models are complementary tools, as results from field experiments permit the development and use of theoretical models in the laboratory. During 1991, we carried out seven sampling campaigns in co-ordination with the Ascó nuclear power plant to collect water samples during the routine release of low-level liquid radioactive waste. Tritium concentrations showed a variation consistent with the detection of a contamination pulse from the plant.

The one-dimensional advection-diffusion equation was solved for the case of a non-instantaneous tracer release. The longitudinal dispersion coefficient and the velocity of the Ebro river waters, together with their respective uncertainties, were determined by the use of three different models: analytical, box-type and numerical. The models presented similar results, with greater similarity between the box-type and the analytical models.

In the Ebro river waters, far-field dispersion had occurred before 50 channel widths downstream from the point source. This value is lower than the range reported by other authors, namely 100 to 300 times the channel width. For the river water flows investigated, ranging from 178 to 915 $m^3 s^{-1}$, longitudinal dispersion coefficients ranged from 41 ± 30 to 392 ± 45 $m^2 s^{-1}$ and mean velocities ranged from 0.563 ± 0.011 to 1.278 ± 0.019 m s^{-1}.

The longitudinal dispersion coefficients determined in this study were similar to those in other rivers of the world with similar characteristics to the Ebro river. The results of this work can be used to predict the displacement and the dispersion of a soluble substance in the Ebro river downstream the nuclear power plant.

NOTATION

$A(x,t)$	mathematical function.
$c(x,t)$	mean cross sectional concentration of the pollutant or tracer, Bq l^{-1}.
$c_{x,t+\Delta t}$	mean cross sectional concentration, as a function of time, for a distance x from the emission point (explicit numerical model), Bq l^{-1}.
c_i^{exp}	experimental tritium concentration, Bq l^{-1}.
c_i^{the}	theoretical tritium concentration for one model, Bq l^{-1}.
C_i	background concentration of the tracer, Bq l^{-1}.
C_0	initial mean cross sectional concentration after total mixing, Bq l^{-1}.
C_t	mean concentration of tracer release, Bq l^{-1}.
d	mean depth, m.
D	longitudinal dispersion coefficient, m^2 s^{-1}.
D_o	optimized longitudinal dispersion coefficient, m^2 s^{-1}.
erfc(x)	complementary error function.
F_i	experimental data for chi–square fitting.
I	dimensionless parameter.
k_b	dispersion coefficient in the box–type model, m^2 s^{-1}.
k_b'	numerical dispersion coefficient in the box–type model, m^2 s^{-1}.
$k_{i,1}$	transfer coefficient from compartment i to compartment i+1, s^{-1}.
$k_{i,2}$	transfer coefficient from compartment i to compartment i-1, s^{-1}.
k_z	transverse dispersion coefficient, m^2 s^{-1}.
L	mixing length, m.
n	number of experimental observations.

N_i tracer particles in box i.

q tracer release flow rate, $m^3\ s^{-1}$.

Q river discharge, $m^3\ s^{-1}$.

$Q_i(t)$ tracer sources, tracer particles s^{-1}.

r pipe radius, m.

s^2 variance.

S_i surface of compartment i, m^2.

t time, s.

Δt temporal resolution of the box–type and numerical models, s.

u' velocity deviation, m s^{-1}.

$\overline{u'^2}$ mean square velocity deviation, $m^2\ s^{-2}$.

u^* shear velocity, m s^{-1}.

v mean flow velocity, m s^{-1}.

v_o optimized velocity, m s^{-1}.

V_i volume of compartment i, m^3.

w channel width, m.

W derivative of a function with respect the parameters estimate (matrix).

W' transpose of the matrix W.

$(W'W)^{-1}$ covariance matrix.

x cartesian coordinate in the flow direction, m.

x_i independent variable.

Δx spatial resolution of the box–type and numerical models, m.

Δx_i length of the compartment i, m.

y_i dependent variable.

$\hat{y}_i$	estimate value of the dependent variable.
α	parameter estimated in a model.
β	parameter estimated in a model.
ε	statistical significance risk level.
χ^2	chi-square.
χ^2_ε	statistically significant χ^2 with a risk level ε.
λ	decay constant, s^{-1}.
ϕ_i	theoretical data for chi–square fitting.
θ_j	general parameter estimated in a model.
σ_α	uncertainty in the α parameter.
σ_β	uncertainty in the β parameter.

ACKNOWLEDGEMENTS

Financial support received from *Junta de Sanejament de la Generalitat de Catalunya* is gratefully acknowledged. Also, we wish to express our gratitude to the Ascó nuclear power plant for its collaboration in this study and by facilitating important information for its scientific development. Thanks are due to our colleagues in the Physics Department for their collaboration in sampling campaigns.

REFERENCES

Abramowitz, M. & Stegun, I.A. (1972). *Handbook of Mathematical Functions*. Dover Publications, Inc., New York, pp. 316.

Abril, J.M. & García León, M. (1992). A marine dispersion model for radionuclides and its calibration from non-radiological information. *J. Environ. Radioactivity*, **16**, 127-46.

APHA-AWWA-WEF (1992). *Standard Methods for the Examination of Water and Wastewater*. American Public Health Association, Washington.

Beltaos, S. (1980). Longitudinal dispersion in rivers. *J. Hydraul. Div.*, **106**, 151-72.

Clark, J.F., Schlosser, P., Stute M. & Simpson H.J. (1996). SF_6-He-3 tracer release experiment: a new method of determining longitudinal coefficients in large rivers. *Environ. Sci. Technol.*, **30**, 1527-32.

Cuadras, C.M. (1991). *Problemas de Probabilidad y Estadística.* Volumen 2, Promociones y Publicaciones Universitarias S.A., Barcelona (in Spanish).

Currie, L.A. (1968). Limits for qualitative detection and quantitative determination. *Analytical Chemistry*, **40**, 586-92.

Day, T.J. (1975). Longitudinal dispersion in natural channels. *Water Resour. Res.*, **11**, 909-18.

Day, T.J. (1977). Observed mixing lengths in mountain streams. *J. Hydrology*, **35**, 125-36.

Eisenbud, M. (1987). *Environmental Radioactivity*. Academic Press, New York..

Elder, J.W. (1959). The dispersion of marked fluid in turbulent shear flow. *J. Fluid Mech.*, **12**, 544-60.

Fischer, H.B. (1973). Longitudinal dispersion and turbulent mixing in open-channel flow. *Ann. Rev. Fluid Mech.*, **5**, 59-78.

Gordon, N.D., McMahon, T.A. & Finlayson, B.L. (1992). Stream Hydrology. John Wiley and Sons, Chichester.

Graf, J.B. (1995). Measured and predicted velocity and longitudinal dispersion at steady and unsteady flow, Colorado River, Glen Canyon dam to lake Mead. *Water Resour. Bull.*, **31**, 265-81.

Guizerix, J. & Florkowski, T. (1983). Streamflow measurements. In *Guidebook on Nuclear Techniques in Hydrology*. Technical reports series, No. 91, International Atomic Energy Agency, Vienna, pp. 65-79.

IAEA (International Atomic Energy Agency) (1985). *Hydrological Dispersion of Radioactive Material in Relation to Nuclear Power Plant Siting*. Safety Series No. 50-SG-S6, IAEA, Vienna.

ISO (International Organization for Standardization) (1987). *Mesure de débit des liquides dans les canaux découverts - Méthodes de dilution pour le mesurage du débit en régime permanet*. ISO 555-2, ISO, Switzerland (in French).

Keith, L. H., Crummett, W., Deegan, J., Libby, R. A., Taylor, J. K., Wentler, G. & ACS Committee on environmental improvement (1983). Principles of Environmental

Analysis. *Anal. Chem*., **55**, 2210-8.

Kincaid, D. & Cheney, W. (1991). *Numerical Analysis*. Wadsworth, Inc., California.

Knighton, D. (1984). *Fluvial Forms and Processes*. Edward Arnold, London.

Knopman, D.S. & Voss, C.I. (1987). Behaviour of sensitivities in the one-dimensional advection-dispersion equation: implications for parameter estimation and sampling design. *Water Resour. Res.*, **23**, 253-72.

Lebreton, J.C. (1974). *Dynamique Fluviale*. Eyrolles, Paris.

Morisawa, M. (1985). *Rivers*. Longman Group Limited, New York.

Mossman, D.J., Holly, F.M. & Schnoor, J.L., (1991). Field observations of longitudinal dispersion in a run-of-the-river impoundment. *Wat. Res.*, **25**, 1405-15.

Myers, R.H. (1986). *Classical and Modern Regression with Applications*. PWS Publishers, Boston, Massachusetts.

Nordin, C.F. & Troutman, B.M. (1980). Longitudinal dispersion in rivers: the persistence of skewness in observed data. *Water Resour. Res.*, **16**, 123-28.

Noye, J. (1987). Finite difference methods for solving one-dimensional transport equation. In *Numerical Modelling: Applications to Marine Systems*, ed. J. Noye. Elsevier Science Publishers B.V., North-Holland, pp. 231-56.

Prandle, D. (1984). A modelling study of the mixing of ^{137}Cs in the seas of the european continental shelf. *Phil. Trans. R. Soc. Lond.* A **310**, 407-36.

Press, W.H., Flannery, B.P., Teukolsky, S.A. & Vetterling, W. T. (1986). *Numerical Recipes*. Cambridge University Press, Cambridge, pp. 163-4.

Pujol, Ll. (1996). *Radiactividad del agua superficial y los sedimentos en la cuenca del Ebro. Utilización del tritio como radiotrazador en el tramo catalán*. Ph.D., Universitat Autònoma de Barcelona (in Spanish).

Rawlings, J.O. (1988). *Applied Regression Analysis: A Research Tool*. Wadsworth, Inc.,

California.

Rutherford, J.C. (1994). *River mixing*. John Willey & Sons, Chichester, England.

Sanchez-Cabeza, J.A., Pujol, Ll., Molero, J., Merino, J., León, L., Vidal-Quadras, A., Schell, W.R., Trilla, J. & Mitchell, P.I. (1992). Estudio preliminar sobre el transporte de especies químicas solubles en el río Ebro utilizando el tritio como trazador. En *Actas de la XVIII Reunión de la Sociedad Nuclear Española*, Madrid, Sección 2.05 (in Spanish).

Scott, E.M. (1994). Simple environmental models for radioactive dispersal in the marine environment. En *Low-Level Measurements of Radioactivity in the Environment. Techniques and Applications*, ed. M. García-León & R. García-Tenorio. World Scientific, Singapore, pp. 447-60.

Van Genuchten, M.T. & Alves, W.J. (1982). Analytical solutions of the one-dimensional convective-dispersive solute transport equation. *U.S. Dep. of Agric. Tech. Bull.*, Nº 1661, 9.

Whicker, F.W. & Schultz, V. (1982). *Radioecology: Nuclear Energy and the Environment*. CRC Press Inc., Boca Ratón, Florida.

Yotsukura, N. & Sayre, W.W. (1976). Transverse mixing in natural channels. *Water Resour. Res.*, **12**, 695-704.

Yu, Yun-Sheng & Wenzhi, L. (1989). Longitudinal dispersion in rivers: a dead-zone model solution. *Water Resour. Bull.*, **25**, 319-25.

TABLE 1

Characteristics of the tritium releases from Ascó nuclear power plant monitored in this work (Asociación Nuclear Ascó, personal communication, 1991)

Date (1991)	Release start	Release duration (min)	Volume released (m^3)	Tritium activity (GBq m^{-3})	Mixing activity† (Bq l^{-1})
May 6	11:40	110	19.80	6.88	22.6
July 15	10:28	126	22.68	0.85	14.3
August 5	09:43	67	23.00	2.06	56.0
December 5	10:15	60	20.33	13.8	124
December 9	14:20	42	16.31	13.6	226
December 13	10:16	49	19.80	0.52	9.7
December 16	10:28	72	26.40	12.5	219

†Activity concentrations at full mixing were derived from eqn (1).

TABLE 2

Sampling information

Date (1991)	Sampling location[†]	Latitude (N)	Longitude (E)	Distance[‡] (km)	Sampling period	River discharge[§] (m^3 s^{-1})
May 6	Pas de l'Ase	41º 09' 55"	0º 36' 45"	6.5	12:00 - 17:00	915
July 15	García	41º 08' 15"	0º 38' 55"	11.0	14:45 - 19:00	178
August 5	Mora de Ebro	41º 05' 55"	0º 38' 30"	16.0	15:30 - 19:15	211
Dec. 5	Mora de Ebro	41º 05' 55"	0º 38' 30"	16.0	13:30 - 18:30	626
Dec. 9	Ascó	41º 11' 05"	0º 34' 20"	0.5	13:00 - 17:00	390
Dec. 13	García	41º 08' 15"	0º 38' 55"	11.0	13:15 - 17:45	359
Dec. 16	Miravet	41º 02' 00"	0º 36' 35"	28.0	16:30 - 23:30	348

[†]See Fig. 1.

[‡]From Ascó nuclear power plant.

[§] Flix dam, personal communication.

TABLE 3

Comparison between the total amount of tritium released by the Ascó nuclear power plant and the total amount that passed by a sampling location

Date (1991)	Sampling location	Distance† (km)	Total tritium activity (GBq)	Total tritium activity passed by the sampling location (GBq)
May 6	Pas de l'Ase	6.5	136	118 ± 5
July 15	García	11.0	19.2	20.0 ± 0.8
December 5	Mora de Ebro	16.0	280	227 ± 3
December 9	Ascó	0.5	222	28.9 ± 1.4‡
December 13	García	11.0	10.3	9.0 ± 0.7
December 16	Miravet	28.0	329	283 ± 2

Uncertainties correspond to ± 1σ.

† From Ascó nuclear power plant.

‡ See Discussion section .

TABLE 4

Summary of the optimised parameters determined with the different models

Location	Model	v ($m\ s^{-1}$)	D ($m^2\ s^{-1}$)	χ^2	$\chi^2_{0.05}$
Pas de l'Ase	Analytical	1.247 ± 0.017	101 ± 26	0.8	14.1
(May 6, 1991)	Box-type	1.278 ± 0.019	104 ± 27	0.9	14.1
	Numerical	1.247 ± 0.017	175 ± 26	0.9	14.1
García	Analytical	0.563 ± 0.011	48 ± 18	9.8	21.0
(July 15, 1991)	Box-type	0.567 ± 0.011	48 ± 18	9.7	21.0
	Numerical	0.558 ± 0.011	78 ± 18	9.7	21.0
Mora de Ebro	Analytical	1.119 ± 0.015	218 ± 34	35.2	21.0
(Dec. 5, 1991)	Box-type	1.146 ± 0.015	222 ± 36	36.3	21.0
	Numerical	1.119 ± 0.015	283 ± 34	35.3	21.0
García	Analytical	0.847 ± 0.027	41 ± 30	5.0	7.8
(Dec. 13, 1991)	Box-type	0.852 ± 0.028	42 ± 31	4.9	7.8
	Numerical	0.844 ± 0.027	89 ± 31	4.9	7.8
Miravet	Analytical	0.858 ± 0.011	379 ± 45	88.6	38.9
(Dec. 16, 1991)	Box-type	0.884 ± 0.011	392 ± 45	87.6	38.9
	Numerical	0.860 ± 0.010	376 ± 36	97.8	38.9

Uncertainties correspond to ± 1σ.

TABLE 5

Reported longitudinal dispersion coefficients for rivers with similar characteristics to the Ebro river (Rutherford, 1994)

River	Mean depth (m)	Mean width (m)	Mean velocity (m s^{-1})	Discharge (m^3 s^{-1})	Dispersion coefficient (m^2 s^{-1})
Missouri	2.70	200	1.55	837	1500
	2.33	183	0.89	380	465
Sabine	2.04	104	0.58	119	316
	4.75	128	0.64	389	670
Yadkin	2.33	70	0.43	71	111
	3.85	72	0.76	213	260
Waikato	2.60	85	0.69	153	52
	2.00	120	0.64	153	67
Ebro[†]	*2.4 - 3.0*	*120 - 140*	*0.56 - 1.28*	*178 - 915*	*41 - 392*

[†] This work.

Figure Captions

Fig. 1. Map of the studied Ebro river section showing sampling locations.

Fig. 2. Tritium concentration as a function of time after some low-activity liquid radioactive waste releases from Ascó nuclear power plant during 1991. (A) Pas de l'Ase, May 6; (B) García, July 15; (C) Mora de Ebro, August 5; (D) Mora de Ebro, December 5; (E) Ascó, December 9; (F) García, December 13; (G) Miravet, December 16. The solid line shows the optimum analytical model fit and (•) the experimental data.

Fig. 3. Dependence of the Ebro river waters mean velocity with discharge (analytical model).

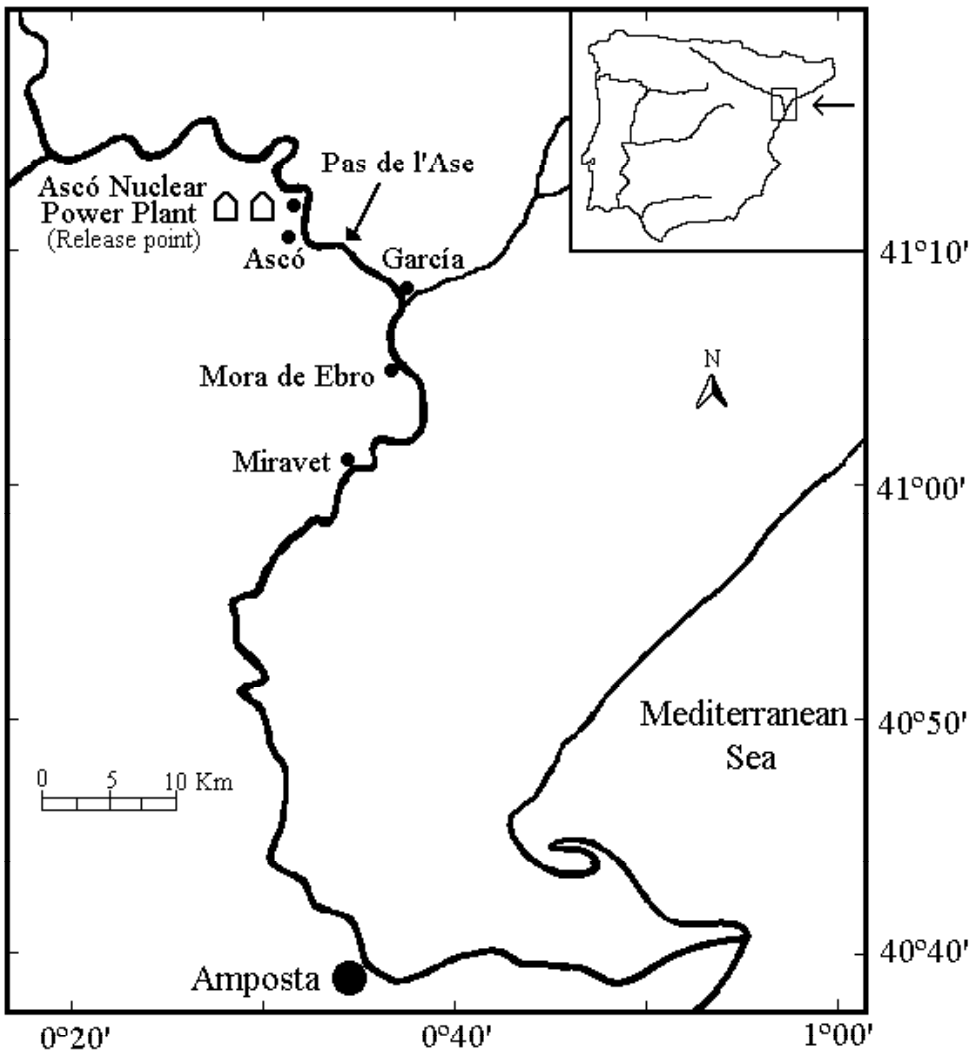
Pas de l'Ase
Ascó Nuclear
Power Plant
(Release point)
Ascó
García
Mora de Ebro
Miravet
Amposta
Mediterranean
Sea
N
0 5 10 Km
41°10'
41°00'
40°50'
40°40'
0°20'
0°40'
1°00'

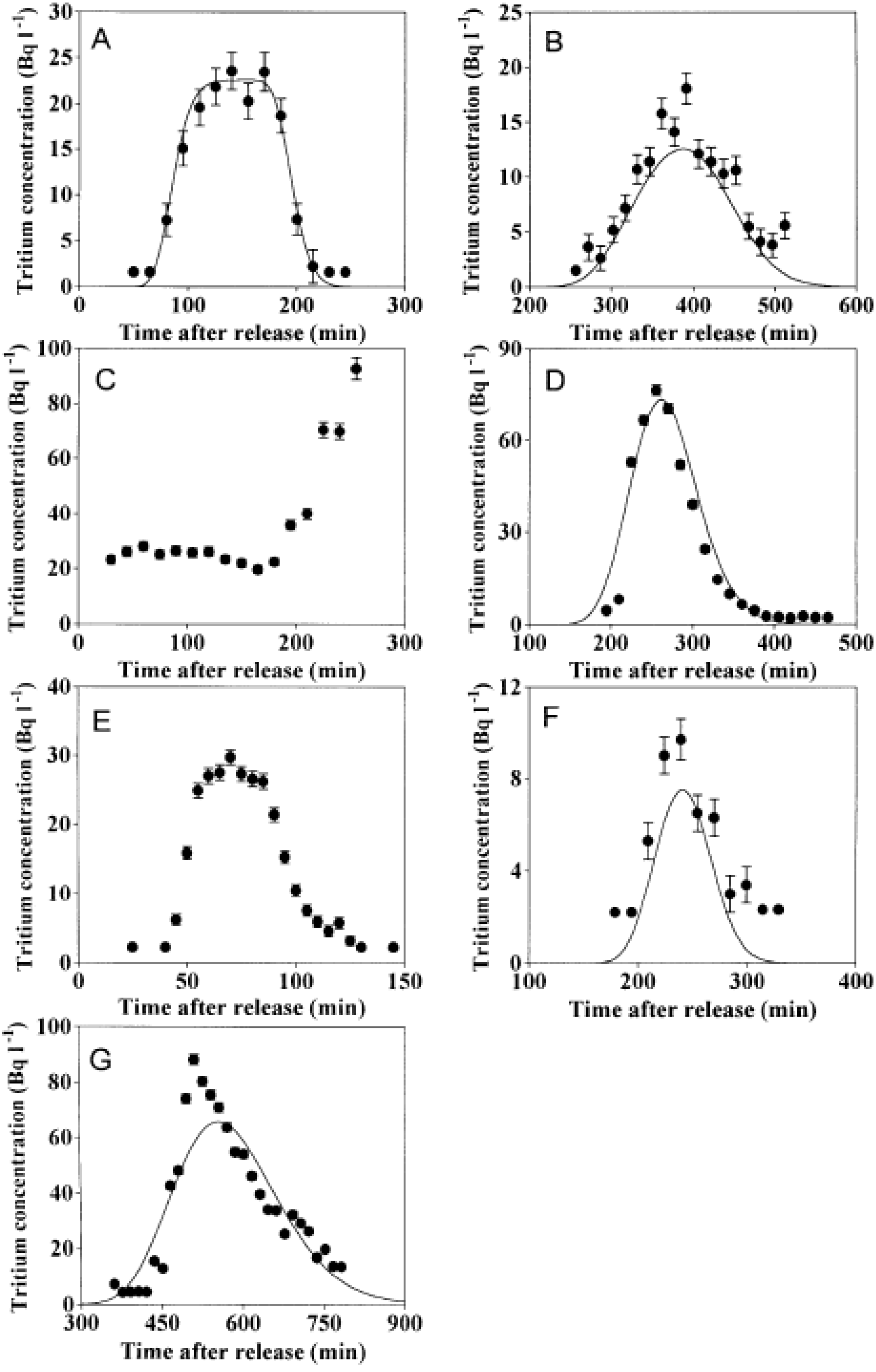
A
Tritium concentration (Bq l-1)
Time after release (min)
B
Tritium concentration (Bq l-1)
Time after release (min)
C
Tritium concentration (Bq l-1)
Time after release (min)
D
Tritium concentration (Bq l-1)
Time after release (min)
E
Tritium concentration (Bq l-1)
Time after release (min)
F
Tritium concentration (Bq l-1)
Time after release (min)
G
Tritium concentration (Bq l-1)
Time after release (min)

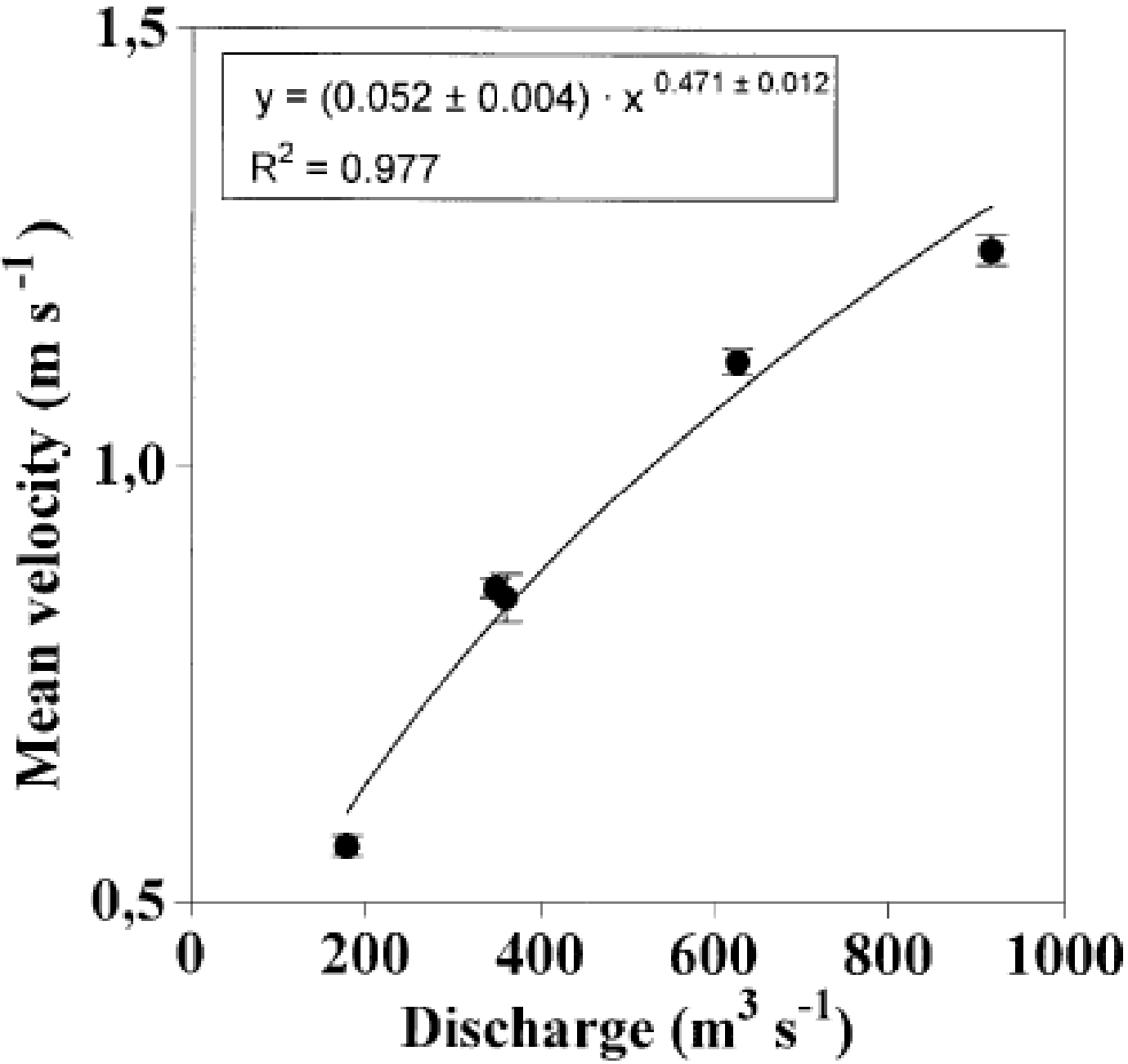
y = (0.052 ± 0.004) · x 0.471 ± 0.012
R2 = 0.977
1,5
1,0
0,5
Mean velocity (m s-1)
0
200
400
600
800
1000
Discharge (m3 s-1)